Alkaline aqueous solution of sodium decahydro-closo-decaborate Na2B10H10 as liquid anodic fuel

Salem Ould-Amara, Eddy Petit, Dominique Granier, Pascal Yot, Umit Demirci

Alkaline aqueous solution of sodium decahydro-*closo*-decaborate $Na_2B_{10}H_{10}$ as liquid anodic fuel

Salem OULD-AMARA,[1] Eddy PETIT,[2] Dominique GRANIER,[2] Pascal G. YOT,[2] Umit B. DEMIRCI[1,*]

[1] Institut Européen des Membranes, IEM – UMR 5635, ENSCM, CNRS, Univ Montpellier, Montpellier, France

[2] Institut Charles Gerhardt Montpellier, ICGM – UMR 5253, CNRS, ENSCM, Univ Montpellier, Montpellier, France

*Corr. author: umit.demirci@umontpellier.fr

Abstract

The potential of the decahydro-*closo*-decaborate anion $B_{10}H_{10}^{2-}$ in alkaline aqueous solution as anodic fuel was investigated by using cyclic voltammetry and three different bulk metal electrodes (platinum, gold and silver). The sodium salt $NaB_{10}H_{10}$ was first synthesized, fully characterized and assessed for its relative stability in alkaline medium for 25 days. Then, oxidation of $B_{10}H_{10}^{2-}$ in alkaline aqueous solution was studied. With platinum, the electrochemical activity is nil. With gold and silver, oxidation takes place at >0 V *vs*. SCE, suggesting direct oxidation of $B_{10}H_{10}^{2-}$. A current density of *e.g.* 15.1 mA cm^{-2} at 0.51 V *vs*. SCE is produced, supporting an electrocatalytically activity for both electrodes. There is even some reversibility of the process (*i.e.* reduction of intermediate species) with silver. The most important oxidation products were identified as being B_7-based anions for both silver and gold. Such results suggest the occurrence of partial oxidative degradation of $B_{10}H_{10}^{2-}$ at positive potential and may open new application prospects to polyborate anions.

Keywords

Anodic liquid fuel; Boron cluster; $Na_2B_{10}H_{10}$; Oxidation; Polyborate anion; Sodium decahydro-*closo*-decaborate

1. Introduction

In the recent decades huge efforts have been dedicated to the development of a wide variety of materials for energy/hydrogen storage [1], including boron hydrides [2]. A typical and early example is sodium borohydride $NaBH_4$, much investigated for hydrogen storage [3] and as anodic fuel for chemical energy storage [4]. A more recent example is sodium dodecahydro-*closo*-dodecaborate $Na_2B_{12}H_{12}$. It belongs to the family of the polynuclear borane anion-based salts [5], which have been considered: (*i*) for hydrogen storage and production (by hydrolysis) [6]; (*ii*) as anodic fuel for chemical energy storage [7]; and (*iii*) as solid electrolyte in electrochemical energy storage [8].

Both of the aforementioned boron hydrides have been considered as potential carbon-free anodic fuels owing to their solubility and relative stability in water. With respect to the borohydride anion BH_4^-, it spontaneously hydrolyzes when put into contact with water, which results in hydrogen evolution [9]:

$$BH_4^- + 4H_2O \rightarrow B(OH)_4^- + 4H_2 \quad (1)$$

The reaction can be drastically limited by increasing the solution pH up to 10-13 [10]. The as-obtained alkaline aqueous solution of BH_4^- is then an attractive anodic fuel ($E° = -1.24$ V) [11]:

$$BH_4^- + 8OH^- \rightarrow BO_2^- + 6H_2O + 8e^- \quad (2)$$

The resulting open circuit potential is as high as 1.64 V. A lot of efforts have been made to develop the related direct borohydride fuel cell technology but the progression objectives have been impeded by several critical issues [12]. One of the main problems relates to the unwanted hydrolysis reaction. It very slowly takes place even in alkaline conditions [10], but more critically it catalytically takes place over the metal electrode [13,14]. One of the main challenges ahead is to better understand the oxidation and hydrolysis mechanisms in order to search for novel anode electrocatalysts allowing depressed hydrogen evolution and making the electro-oxidation of BH_4^- an eight- or near-eight-electron process [15].

Alternatively, other boron hydrides, most being derivatives of $NaBH_4$ [2], have been considered. For example, oxidations of alkaline aqueous solutions of ammonia borane NH_3BH_3, dimethylamine borane $(CH_3)_2HNBH_3$, hydrazine borane $N_2H_4BH_3$ and hydrazine *bis*borane

$N_2H_4(BH_3)_2$ over carbon-supported platinum and palladium nanoparticles were investigated and the boranes were compared each other [16]:

$$XBH_3 + 6OH^- \rightarrow XH^+ + BO_2^- + 4H_2O + 6e^- \quad (3)$$

where X is equal to NH_3, N_2H_4 and $NH(CH_3)_2$. For each of the boranes, oxidation is in competition with heterogeneous hydrolysis, the H_2 evolution being more important over the platinum electrode. Another potential boron hydride is the octahydrotriborate anion $B_3H_8^-$ [17]:

$$B_3H_8^- + 20OH^- \rightarrow 3BO_2^- + 14H_2O + 18e^- \quad (4)$$

It oxidizes over a bulk gold electrode but the effective number of electrons is about 10 out of a theoretical total of 18 electrons (Eq. 4). Complete oxidation is not effective because heterogeneous hydrolysis. A last potential boron hydride was recently proposed. Oxidation of the dodecahydro-*closo*-dodecaborate anion $B_{12}H_{12}^-$ was studied with platinum, gold and silver electrodes [7]. The anion was chosen owing to its high stability in aqueous solution at any pH (no hydrolysis). Partial oxidative degradation through a complex oxidation process was evidenced. One of the products was identified as being $B_{11}H_{11}O(OH)^-$ and its formation was tentatively suggested to take place as follows:

$$B_{12}H_{12}^{2-} + 8OH^- \rightarrow B_{11}H_{11}O(OH)^- + B(OH)_4^- + 2H_2O + 6e^- \quad (5)$$

The most attractive feature with $B_{12}H_{12}^-$ is the absence of heterogeneous hydrolysis. The evolving electrons are all due to partial oxidation of the anion.

The recent achievements briefly described above created a window of opportunity for alkaline aqueous solutions of polynuclear borane anions as possible anodic fuels. In the present work we examined the potential of the decahydro-*closo*-decaborate anion $B_{10}H_{10}^{2-}$ because, after the anion $B_{12}H_{12}^{2-}$, it is the second most stable species against hydrolysis [18]. The sodium salt, *i.e.* $Na_2B_{10}H_{10}$, was synthesized and the successful synthesis and the purity of the sample were verified. Its stability in aqueous solution was investigated so as to launch oxidation experiments. Herein is reported, for the first time, the oxidation behavior of the anion $B_{10}H_{10}^{2-}$ with platinum, gold and silver bulk electrodes.

2. Material and Methods

$Na_2B_{10}H_{10}$ was prepared from the commercially available triethylammonium decahydro-*closo*-decaborate of formulae $((C_2H_5)_3NH)_2B_{10}H_{10}$ (Katchem, 98%) by cationic substitution in alkaline medium:

$$((C_2H_5)_3NH)_2B_{10}H_{10} + 2NaOH \rightarrow Na_2B_{10}H_{10} + 2((C_2H_5)_3NH)OH \quad (6)$$

The synthesis was performed under argon atmosphere. A 2-gram aliquot of $((C_2H_5)_3NH)_2B_{10}H_{10}$ was dispersed in 100 mL of an alkaline aqueous (0.13 M NaOH) solution at room temperature. The suspension was heated at 90°C for 2 h, resulting in the formation of a clear solution. A white powder consisting of $Na_2B_{10}H_{10}$ was recovered by water extraction under vacuum.

The molecular structure of $Na_2B_{10}H_{10}$ was analyzed by Fourier-transform infrared spectroscopy (FTIR; Nicolet™ IS50 Thermo Fisher Scientific; 32 scans), nuclear magnetic resonance (NMR; Bruker AVANCE-300; ^1H such as probe head dual ^1H, 300.13 MHz, CD_3CN, and 30 °C; ^{11}B such as probe head BBO10, 79.39 MHz, D_2O, 30 °C). The crystal structure of $Na_2B_{10}H_{10}$ was analyzed by X-ray powder diffraction (XRPD) using a PANalytical X'Pert diffractometer equipped with an X'Celerator detector Si (111) monochromator. An operation voltage of 40 kV and an intensity of 40 mA were imposed to deliver the wavelength Cu-$K_{\alpha 1}$: λ = 1.54059 Å. The thermal stability of $Na_2B_{10}H_{10}$ was analyzed by thermogravimetric analysis (TGA; TA Instruments Q500; aluminum crucible of 40 µL, heating rate 5°C min^{-1}, under N_2 flow of 60 mL min^{-1}) as well as differential scanning calorimetric (DSC; TA Instruments 2920 MDSC; conditions identical to the TGA experiment).

The oxidation of the anion $B_{10}H_{10}^{2-}$ (of $Na_2B_{10}H_{10}$ in aqueous solution) was studied by cyclic voltammetry (with a µAutolab® Type III potentiostat). A borosilicate cell of 100 mL was used (thermostated at 20°C). It was systematically, and before each experiment, cleaned with peroxymonosulfuric acid H_2SO_5 (Caro's Acid). Outgassed Milli-Q Water (18.2 MΩ cm, < 3 ppb total organic carbon) was used. The electrodes were as follows: saturated calomel electrode (SCE) as reference electrode; platinum wire as counter electrode; and a rotating disk (with bulk platinum ∅ 2 mm, or bulk gold ∅ 2 mm, or bulk silver ∅ 4 mm) as working electrode. We selected platinum, gold and silver because, historically, they have been among the most

investigated metals for oxidation of the anion BH_4^- [12-15]; otherwise, we use to consider these metals only, for screening any new B-based anodic fuel, since we well know about their catalytic behavior towards the unwanted hydrolysis of BH_4^-. The surface of the working electrodes was polished with diamond paste. The electrolyte solution was prepared from an aqueous solution of NaOH at the concentration of 0.1 M. The concentration of $B_{10}H_{10}^{2-}$ was 0.001 M; it was kept so low to limit the interactions between the molecules. The cell voltage range was fixed as follows: −1.05 to +0.6 V *vs*. SCE (in order to avoid water splitting).

Mass spectrometry (MS) experiments allowed qualitative analyses of the oxidation by-products. A Quattro Micro mass spectrometer, with electrospray ionization in negative mode (from Waters Micromass; Wythenshawe, Manchester, UK) and operating at constant flow rate (0.25 mL min^{-1}) was used. The electrolyte samples taken were analyzed by direct injection (Waters 2695 pump-autosampler, with 5 µl loop). A mixture of water and acetonitrile (50/50 in vol. %) was used as mobile phase. The nebulizer gas was N_2. For detection, the conditions were: capillary potential of 3.5 kV; cone potential of 30 V; source temperature at 120°C; desolvation temperature at 450°C; cone gas flow of 50 L h^{-1}; desolvation gas flow of 450 L h^{-1}. The recorded *m*/*z* values were compared to comparable molecular weights (of polyborate anions) and then the experimental spectra were compared to modeled/calculated spectra in order to confirm the identifications made.

3. Results and discussion

3.1. Characterizations of $Na_2B_{10}H_{10}$

The ^{11}B NMR spectrum of the anion $B_{10}H_{10}^{2-}$ (**Figure 1**) shows two doublets centered at −1 ppm (J_{BH} = 140.1 Hz) and −29 ppm (J_{BH} = 125.4 Hz), suggesting two kinds of boron environments in the molecule (2 equivalent apical boron atoms + 8 equivalent equatorial boron atoms) [19]. The relative area of these doublets is 4 to 1, which is in good agreement with the equatorial 8 boron atoms and the 2 apex boron atoms [20,21]. The purity of the sample is also confirmed.

The ^{1}H NMR spectrum of the anion $B_{10}H_{10}^{2-}$ (**Figure 2**) is characterized by several signals, apart from those due to the solvent H_2O and to CH_3CN present in the deuterated solvent. There are two sets of 7 peaks located between 4 and 2 ppm and between 1 and −1 ppm. They are typical of ^{11}B–H and ^{10}B–H bonds [22,23], and are in good agreement with the presence of two B–H environments in the molecular anion [24]. The relative area of these signals is 4 to 1, in good agreement with the number of hydrogen elements bound to the equatorial 8 boron atoms and to the 2 apex boron atoms.

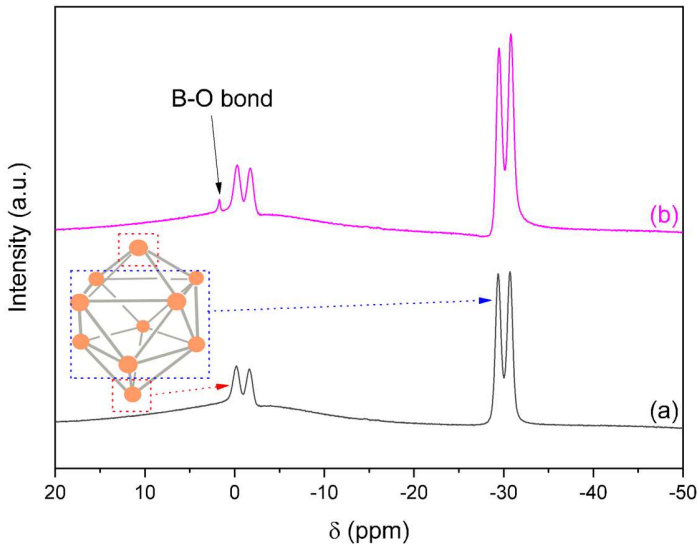

Figure 1. (a) ^{11}B NMR spectrum of the anion $B_{10}H_{10}^{2-}$ (from $Na_2B_{10}H_{10}$). (b) ^{11}B NMR spectrum of the anion $B_{10}H_{10}^{2-}$ in an alkaline solution (1 M NaOH) after 25 days.

Analysis by FTIR spectroscopy was lastly performed on $Na_2B_{10}H_{10}$ (**Figure 3**). The vibration bands at 2432 and 2461 cm^{-1} are favorably ascribed to stretching of the apical and equatorial B–H bonds respectively. The bands between 1300 and 1050 cm^{-1} are due to the B–H bonds deformation. The B–B bonds are featured by the band peaking at 1026 cm^{-1}. This is in good agreement with the fingerprint of the molecular structure of $B_{10}H_{10}^{2-}$ [21,24]. There are additional bands at 3600-3500 and 1604 cm^{-1} that are ascribed to O–H bonds. The presence of B–O–H environments (like in borates) is discarded by the NMR results presented above. These signals may be ascribed to residual and/or adsorbing water molecules.

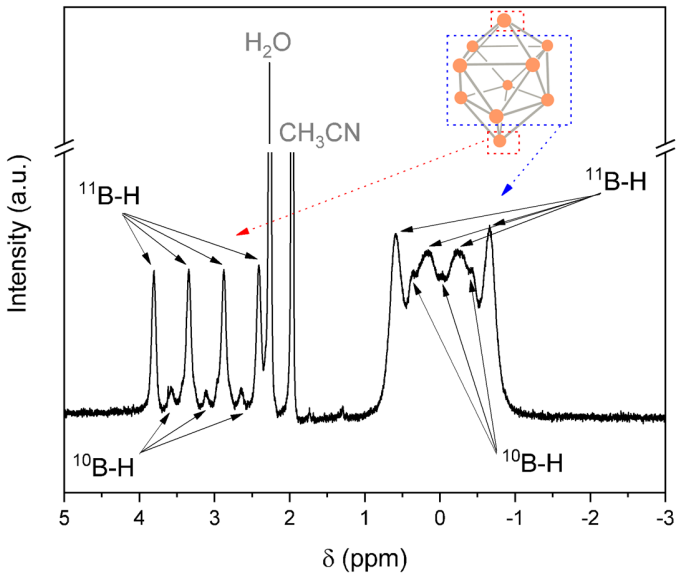

Figure 2. ^{11}H NMR spectrum of the anion $B_{10}H_{10}^{2-}$ (from $Na_2B_{10}H_{10}$).

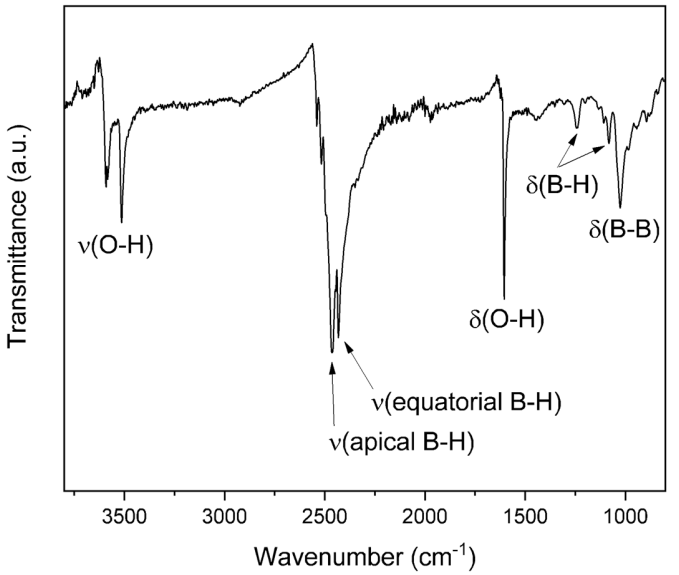

Figure 3. FTIR spectrum of $Na_2B_{10}H_{10}$.

Based on the FTIR observations, the thermally stable $Na_2B_{10}H_{10}$ was analyzed by TGA and DSC (**Figure 4**). Under heating, the sample suffers a first weight loss (1 wt%) up to 50°C and a second one, more important (9.6 wt%), between 100 and 160°C. The latter is featured by an endothermic process. The weight losses are much likely due to removal of adsorbed water as reported elsewhere [25]. The overall weight loss was considered to calculate the number of adsorbed water molecule per mole of $Na_2B_{10}H_{10}$. It was found about to be 1, suggesting the empirical formulae $Na_2B_{10}H_{10}{\cdot}H_2O$.

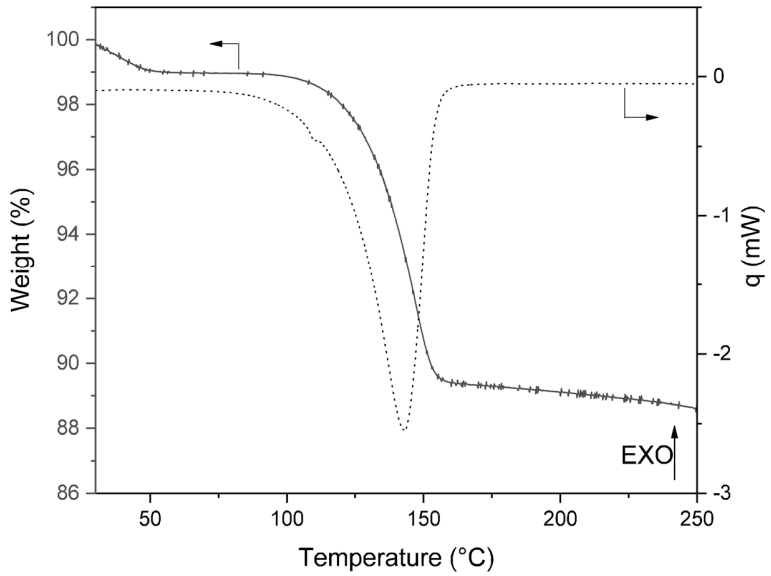

Figure 4. TGA and DSC results for $Na_2B_{10}H_{10}$.

$Na_2B_{10}H_{10}{\cdot}H_2O$ is a white solid. Following the results obtained by TGA and DSC, the powder was placed into a 1 mm diameter glass capillary into a glove box then heat-treated at 110°C overnight under primary vacuum (to remove the residual water molecules) and then sealed to protect the as-obtained anhydrous $Na_2B_{10}H_{10}$ from hydration. The XRPD pattern of the sample was finally recorded in the 2θ range 5°-100° using the Debye-Scherrer method (**Figure 5**). The solid is polycrystalline and the pattern is comparable to previously reported results [26,27]. In our case, an impurity supposed to be NaCl (a = 5.639(1) Å, s.g. *Fm-3m* (No. 225)) was fitted using

Le Bail method. **Figure 5** also presents the refinement of the pattern obtained using JANA2006 software [28]. The crystal structure was successfully solved in the monoclinic phase (Z = 4), using the space group $P2_1/c$ *(No. 14)*. The cell parameters were determined as: a = 6.7228(6) Å; b = 13.1435(11) Å; c = 11.9520(9) Å; β = 120.616(5)°; V = 908.88(13) Å^3 (GoF = 2.08; Rp = 8.62; wRp = 11.47; R(obs)/R(all): 10.06/11.11; wR(obs)/wR(all): 7.66/7.79). The result obtained for the anhydrous phase $Na_2B_{10}H_{10}$ is in good agreement with the work previously reported in ref. [26].

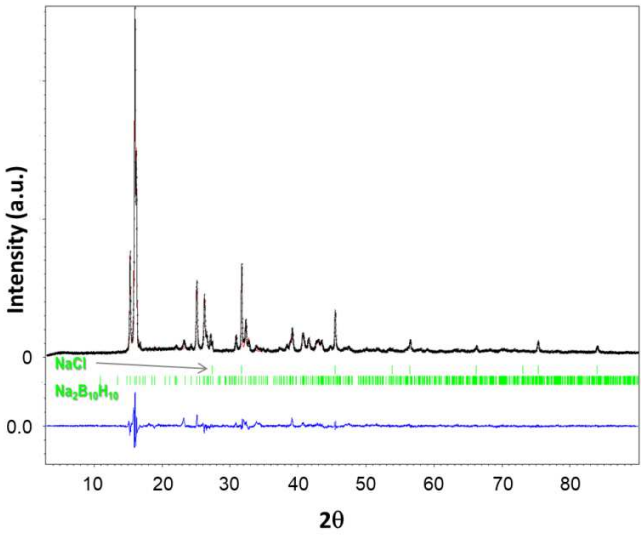

Figure 5. Result of the refinement carried out on the XRPD pattern of anhydrous $Na_2B_{10}H_{10}$ (λ = 1.54059 Å). The observed (in black) and calculated (in red) XRPD profiles for the Rietveld refinement of $Na_2B_{10}H_{10}$ and Le Bail refinement of NaCl are shown. The bottom curve (in blue) is the difference plot on the same scale intensity. The tic marks (in green) are the calculated angles for the Bragg peaks for the two phases in 2θ.

To sum up, $Na_2B_{10}H_{10}\cdot H_2O$ was successfully prepared in our conditions. The sample is monohydrated and contains a small amount of NaCl. This is not problematic for an anodic fuel that has to be dissolved in alkaline aqueous solution. The presence of NaCl had nevertheless to be kept in mind for the preparation of the 0.001 M $Na_2B_{10}H_{10}\cdot H_2O$ solution used as electrolyte.

3.2. Stability of $B_{10}H_{10}^{2-}$ in alkaline solution

As a preliminary step, the stability of $B_{10}H_{10}^{2-}$ (10^{-5} M) in alkaline solution (0.1 M NaOH) was assessed. The fresh solution was analyzed by ^{11}B NMR and then was stored for 25 days before

being analyzed once more by ^{11}B NMR (**Figure 1**). A singlet of small intensity appeared at positive chemical shits (1.7 ppm). It is due to the formation of B–O bonds (by oxidation and/or hydrolysis) like for borates. Despite this, it may be stated that the spectrum indicates a relatively good stability of the anion in the aforementioned conditions. Alkaline solution of $B_{10}H_{10}^{2-}$ is stable enough to be studied as possible anodic fuel.

3.3. Oxidation of $B_{10}H_{10}^{2-}$ over platinum

To our knowledge, oxidation of $B_{10}H_{10}^{2-}$ in alkaline conditions over a metal electrode has not been investigated so far. An example of report available in the open literature deals with chemical oxidation in acidic conditions resulting in the formation of B_{20}-based polynuclear borane anions [29]. Another example is about oxidation by MnO_4^- at pH 7 and at room temperature, resulting in quantitative conversion to boric acid $B(OH)_3$ [30]. Accordingly, the electro-oxidation results reported hereafter were analyzed with the help of the knowledge developed with the anion BH_4^- [12-15,31] and in a lesser extent with the new boron hydride candidates [7,16,17].

The electro-oxidation of $B_{10}H_{10}^{2-}$ was first investigated with the platinum electrode (**Figure 6**) at natural diffusion conditions (0 rpm). The voltammogram does not show apparent oxidation and/or reduction processes. Additional experiments were performed with different rotation rates (up to 2500 rpm) but no marked improvement was observed (voltammograms not reported). Such results do not support bulk platinum as suitable electrode for electro-oxidation of $B_{10}H_{10}^{2-}$. In comparison, the more-stable anion $B_{12}H_{12}^{2-}$ was found to oxidize over the same electrode at <0 V *vs.* SCE, suggesting $B_{12}H_{12}^{2-}$ dissociative adsorption and oxidation of H_{ads}, together with some direct partial oxidation of the anion [7]. The lack of apparent oxidation of $B_{10}H_{10}^{2-}$ could be explained by an absence of adsorption of the anion onto the electrode surface.

3.4. Oxidation of $B_{10}H_{10}^{2-}$ over gold

Gold has been much investigated as effective electrode for oxidation of a boron hydride like $NaBH_4$ [12,15,31]. A bulk gold electrode was also considered in the present work (**Figure 7**). Gold is unable to generate a current below –0.2 V *vs.* SCE. This suggests that it is neither able to partially dissociate $B_{10}H_{10}^{2-}$ [14] nor to valorize adsorbed H species (H_{ads}) [7]. The only

oxidation peak (a_{Au}) appearing during the forward sweep is in the metal-(hydr)oxide region [13], namely at +0.24 V *vs.* SCE for a current density of 3.5 mA cm^{-2}. It may be due to direct (at least partial) oxidation of adsorbed $B_{10}H_{10}^{2-}$ [32]. A similar result was obtained with $B_{12}H_{12}^{2-}$ in similar conditions [7]. For both anions, the process is not reversible. In contrast, in the present work, there is an oxidation peak during the backward sweep: c_{Au} at 0 V *vs.* SCE (0.7 mA cm^{-2}). It is reasonable to suggest oxidation of intermediates (as well as that of $B_{10}H_{10}^{2-}$) [33] and/or oxidation of adsorbed H atoms [34]. Additional experiments were performed at disk rotation rates of 1000 and 2000 rpm (**Figure 7**). The current density for a_{Au} increases up to 4 mA cm^{-2} at 2000 rpm (0.29 V *vs.* SCE). This is an indication of the low impact of poisoning, if it takes place, over the gold electrode [13].

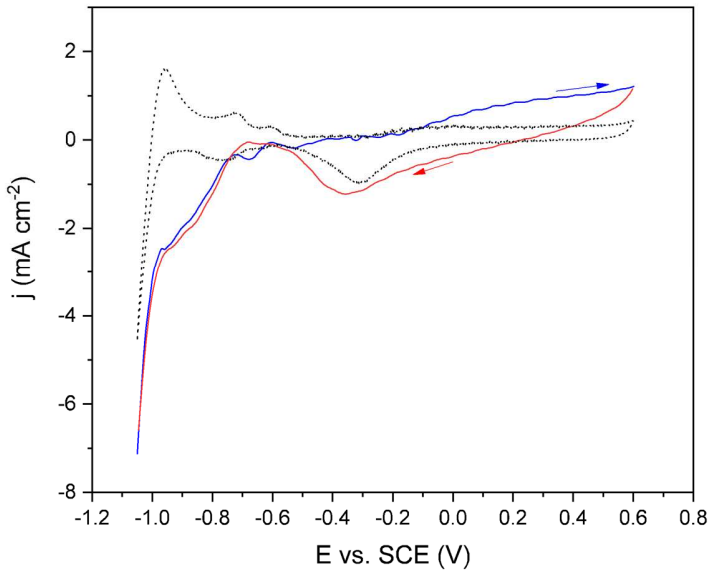

Figure 6. Cyclic voltammogram obtained on bulk platinum at 100 mV s^{-1} and at natural diffusion conditions (0 rpm). The voltammogram of 0.1 M NaOH (dashed lines) is superimposed to that of 0.1 M NaOH + 0.001 M $Na_2B_{10}H_{10}$ (solid lines). The blue line indicates the forward scan and the red line the backward scan, which are besides shown by two arrows.

Because of too low concentrations, the oxidation products could not be identified by ^{11}B NMR [7]. Instead, they were detected and qualitatively analyzed by MS. The CV experiment was repeated while respecting the following procedure: the potential was scanned from –1.05 to +0.6

V *vs.* SCE; there was no negative scan; 1000 successive scans were applied; and, every 100

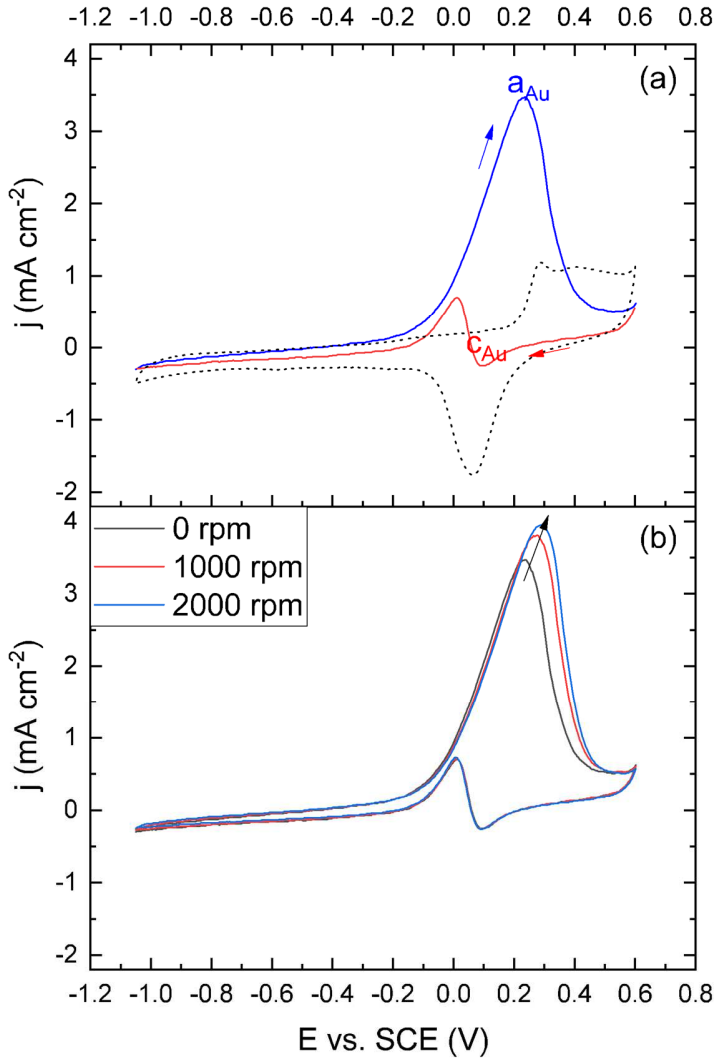

Figure 7. (a) Cyclic voltammogram obtained on bulk gold at 100 mV s^{-1} and at natural diffusion conditions (0 rpm). The voltammogram of 0.1 M NaOH (dashed lines) is superimposed to that of 0.1 M NaOH + 0.001 M $Na_2B_{10}H_{10}$ (solid lines). The blue line indicates the forward scan and the red line the backward scan, which are besides shown by two arrows. (b) Cyclic voltammogram obtained on bulk platinum at 100 mV s^{-1} and at different rotation rates of the disk electrode.

cycles an aliquot of the electrolyte was withdrawn to be analyzed by MS. Several *m/z* values were detected (*m/z* = 69, 99.3, 100.4, 102.3, 116.7), suggesting products formed by partial oxidative degradation of $B_{10}H_{10}^{2-}$ (118 g mol^{-1}). One of them (*m/z* = 99.3) was found to be predominant and it may be ascribed to $B_7H_8O^-$. It is followed by the *m/z* value of 102.3, possibly due to

$B_7H_{11}O^-$. The others were in fact detected in much lesser amounts and their identification has been difficult: the *m/z* values of 100.4 and 116.7 suggest species containing 7 boron atoms (*e.g.* $B_7H_9O^-$ and $B_7H_9O_2^-$); and the *m/z* values of 69 might be ascribed to a species with 4 boron atoms (*e.g.* $B_4H_{10}O^-$). Though the identification of all of the species is difficult, the MS results are thus in good agreement with the CV results implying partial oxidation of $B_{10}H_{10}^{2-}$.

3.5. Oxidation of $B_{10}H_{10}^{2-}$ over silver

Bulk silver was also considered as possible working electrode (**Figure 8**). The forward step is featured by two oxidation peaks: a_{Ag1} at 0.22 V *vs.* SCE with 6.5 mA cm^{-2}, and a_{Ag2} at 0.51 V *vs.* SCE with 15.1 mA cm^{-2}. The first peak is comparable to that observed with the gold electrode and may be attributed to direct (at least partial) oxidation of $B_{10}H_{10}^{2-}$ [32]. With respect to the second oxidation wave, it may be also attributed to direct and possibly more complete oxidation of $B_{10}H_{10}^{2-}$ [35] as well as to oxidation of adsorbed reaction intermediates [33]. The electro-oxidation ability of bulk silver is slightly better than that of bulk gold, making silver a more attractive candidate for further works on electrode materials. With BH_4^-, silver oxide was reported to be the electroactive surface responsible of the direct oxidation of the adsorbed intermediate BH_3OH^- at similar potentials [36]. Surface species such as $Ag(O_xH_yB_z)$ were reported elsewhere [7]. The backward step of the voltammogram shows a reduction (c_{Ag} at –0.15 V *vs.* SCE with –17.6 mA cm^{-2}) of, much likely, an oxidation product. Such a reduction wave let us suggest that the electrochemical process involving $B_{10}H_{10}^{2-}$ and silver is, at least partly, reversible: one (or more) of the species (see below for identified products) forming during the oxidation waves a_{Ag1} and a_{Ag2} is reduced at –0.15 V *vs.* SCE (wave c_{Ag}). The effect of the rotation rate of the disk electrode does not have a negative effect on the current density, which slightly increases along with the higher speed of the rate. Like for the gold electrode, this is an indication of the low impact of poisoning on the surface of bulk silver [13]. Comparable results were obtained with $B_{12}H_{12}^{2-}$ in identical operation conditions but the current densities were 4 times higher (at about 0.5 V *vs.* SCE) [7].

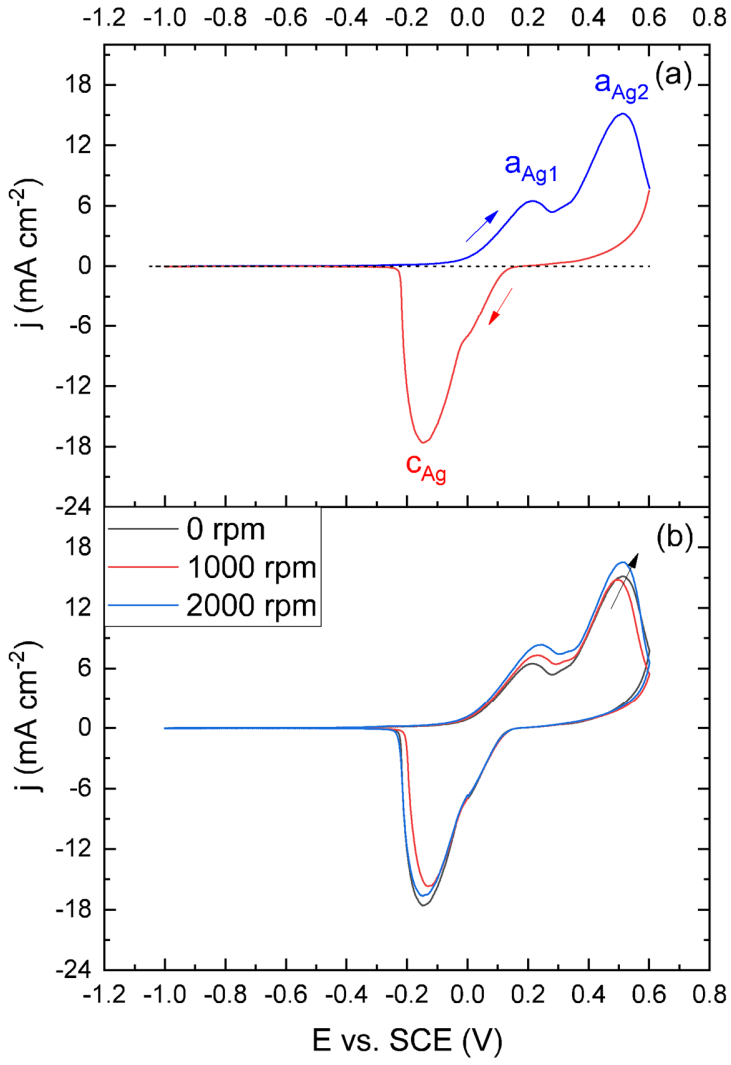

Figure 8. (a) Cyclic voltammogram obtained on bulk silver at 100 mV s^{-1} and at natural diffusion conditions (0 rpm). The voltammogram of 0.1 M NaOH (dashed lines) is superimposed to that of 0.1 M NaOH + 0.001 M $Na_2B_{10}H_{10}$ (solid lines). The blue line indicates the forward scan and the red line the backward scan, which are besides shown by two arrows. (b) Cyclic voltammogram obtained on bulk platinum at 100 mV s^{-1} and at different rotation rates of the disk electrode.

Considering the above-reported cyclic voltammetry performances, the bulk electrodes can be discussed in terms of electrochemical activity. In our conditions, the highest current density was measured for bulk silver (followed by gold), making it the best candidate. Platinum is electrocatalytically inactive. Over silver and gold, the oxidation processes require high potentials (e.g. 0.51 V *vs.* SCE for a_{Ag2} in **Figure 8**) and take place in the metal-oxide region, showing thus the importance of surface (hydr)oxides in oxidation of $B_{10}H_{10}^{2-}$. Though the present results are

mixed, there are interesting and open opportunities for improvement. The potential of alkaline aqueous $B_{10}H_{10}^{2-}$ as anodic fuel would depend on the development of multimetallic electrodes in order to achieve lower oxidation potentials (more realistic for a fuel cell application) and higher current densities (*via* complete oxidation). With the much-investigated BH_4^-, such improvements were reported for *e.g.* Au-Cu [37,38], Ag-Cu [39] and Ag-Pt alloys [40].

The oxidation products forming over bulk silver were analyzed by MS by repeating the CV experiment and following the conditions described for the gold electrode. Several *m*/*z* signals were detected. Only one signal (*m*/*z* = 102.3, ascribed to $B_7H_{11}O^-$) predominated. This species could be that reducing during the backward step of the CV experiment (**Figure 8**). The other *m*/*z* signals could be considered as minor (*m*/*z* = 145, suggested to belong to *e.g.* $B_{11}H_{10}O^-$) or very minor products (*m*/*z* = 100.4 possibly for $B_7H_9O^-$, 116.7 probably due to $B_7H_9O_2^-$, and 142.6 for an unidentified compound). These results clearly indicate the partial oxidative degradation of $B_{10}H_{10}^{2-}$ over the silver electrode and support the CV results discussed above.

4. Conclusion

The potential of the decahydro-*closo*-decaborate anion $B_{10}H_{10}^{2-}$ (in alkaline aqueous solution) as anodic fuel (ultimately for direct liquid-fed fuel cell) was considered and assessed with the help of cyclic voltammetry and by using three different bulk metal electrodes such as platinum, gold and silver. As a first step the sodium salt was synthesized and the obtained white solid was characterized and identified by NMR, FTIR and XRPD. Rather stable in alkaline medium (oxidation in small extent with formation of B–O bonds after 25 days in a solution at 0.1 M NaOH), the anion $B_{10}H_{10}^{2-}$ was found to be suitable for the cyclic voltammetry experiments. With the bulk platinum electrode, the electrochemical activity is nil. In contrast, with bulk gold and silver, oxidation takes place at potentials higher than 0 V *vs.* SCE, suggesting direct oxidation of $B_{10}H_{10}^{2-}$. There is some reversibility of the oxidation process with the silver electrode. Both electrodes are electrocatalytically active and allow the production of current densities (*e.g.* 15.1 mA cm^{-2} at 0.51 V *vs.* SCE) that are however low for the targeted ultimate application. The most important oxidation products were identified by MS. The anion $B_7H_8O^-$

predominates for the gold electrode while $B_7H_{11}O^-$ is the preponderate species for bulk silver. In both cases, the results suggest the occurrence of partial oxidative degradation of $B_{10}H_{10}^{2-}$ at positive potentials. From the present work there are thus three conclusions to be drawn. First, the well-known stability of the polynuclear borane anions is, to a certain extent, confirmed. In our conditions, $B_{10}H_{10}^{2-}$ is stable towards oxidation over bulk platinum and it slightly oxidizes over gold and silver. Second, partial oxidative degradation of $B_{10}H_{10}^{2-}$ over the last two electrodes could be valorized differently, namely by focusing on the synthesis of species like $B_7H_8O^-$ and $B_7H_{11}O^-$ provided novel and advanced electrodes are developed for improved conversion and selectivity. Third, silver appears to the best metal when alkaline aqueous $B_{10}H_{10}^{2-}$ is considered as potential anodic fuel. However, the oxidation potentials are high and the current densities relatively low (in comparison to *e.g.* performance of the much-investigated BH_4^-). Notwithstanding, the anion $B_{10}H_{10}^{2-}$ should not be discarded from the targeted application because of very attractive theoretical properties (*cf.* supplementary information): (*i*) a total oxidation of $B_{10}H_{10}^{2-}$ could generate up to 22 electrons; (*ii*) the theoretical oxidation potential is as low as −3.3 V; and (*iii*) the theoretical specific energy of a fuel cell based on the couple $B_{10}H_{10}^{2-}/O_2$ would be a high as *ca.* 18500 Wh kg^{-1}, which is much higher than the theoretical specific energy of a number of liquid fuels [41]. However further works are necessary to make $B_{10}H_{10}^{2-}$ useable and this calls for developments of silver-based multimetallic electrodes efficiently operating at low potential.

Acknowledgements

This work was supported by the ANR Agence Nationale de la Recherche [program "Investissements d'Avenir", LabEx CheMISyst, grant number ANR-10-LABX-05-01]; the Région Languedoc-Roussillon [program "Chercheur(se)s d'Avenir 2013", project C3, grant number 2013 008555]. We thank Prof. M. Cretin (IEM, Univ Montpellier) for accessibility to cyclic voltammetry.

References

[1] C. Liu, F. Li, H.M. Cheng, Advanced materials for energy storage, Adv. Mater. 22 (2011) E28–E62.

[2] U.B. Demirci, Sodium borohydride for the near-future energy: a “rough diamond” for Turkey, Turk. J. Chem. 42 (2018) 193–220.

[3] P. Brack, S.E. Dann, K.G.U. Wijayantha, Heterogeneous and homogenous catalysts for hydrogen generation by hydrolysis of aqueous sodium borohydride ($NaBH_4$) solutions, Energy Env. Eng. 3 (2015) 174–188.

[4] M.C. Sison Escaño, R.L. Arevalo, E. Gyenge, H. Kasai, Electrocatalysis of borohydride oxidation: a review of density functional theory approach combined with experimental validation, J. Phys.: Condens. Matter 26 (2014) 353001:1–14.

[5] R.E. Williams, The polyborane, carborane, carbocation continuum: architectural patterns, Chem. Rev. 92 (1992) 177–207.

[6] A.V. Safronov, S.S. Jalisatgi, H.B. Lee, M.F. Hawthorne, Chemical hydrogen storage using polynuclear borane anion salts, Int. J. Hydrogen Energy 36 (2011) 234–239.

[7] S. Pylypko, S. Ould-Amara, A. Zadick, E. Petit, M. Chatenet, M. Cretin, U.B. Demirci, The highly stable aqueous solution of sodium dodecahydro-*closo*-dodecaborate $Na_2B_{12}H_{12}$ as a potential liquid anodic fuel, Appl. Catal. B Env. 222 (2018) 1–8.

[8] N. Verdala, J.H. Her, V. Stavila, A.V. Soloninin, O.A. Babanova, A.V. Skripov, T.J. Udovic, J.J. Rush, Complex high-temperature phase transitions in $Li_2B_{12}H_{12}$ and $Na_2B_{12}H_{12}$, J. Sol. State Chem. 212 (2014) 81–91.

[9] M.V. Mirkin, H. Yang, A.J. Bard, Borohydride oxidation at a gold electrode, J. Electrochem. Soc. 139 (1992) 2212–2217.

[10] M.M. Kreevoy, J.E.C. Hutchins, H_2BH_3 as an intermediate in tetrahydridoborate hydrolysis, J. Am. Chem. Soc. 94 (1972) 6371–6376.

[11] M.E. Indig, R.N. Snyder, Sodium borohydride, an interesting anodic fuel, J. Electrochem. Soc. 109 (1962) 1104–1106.

[12] J. Ma, Y. Sahai, Direct borohydride fuel cells – Current status, issues, and future directions, in: L. An, T.S. Zhao (Eds.), Anion exchange membrane fuel cells, Springer International Publishing AG, Cham, 2018, pp. 249–273.

[13] G. Braesch, A. Bonnefont, V. Martin, E.R.Savinova, M. Chatenet, Borohydride oxidation reaction mechanisms and poisoning effects on Au, Pt and Pd bulk electrodes: From model (low) to direct borohydride fuel cell operating (high) concentrations, Electrochim. Acta 273 (2018) 483-494.

[14] P.Y. Olu, A. Bonnefont, G. Braesch, V. Martina, E.R. Savinova, M. Chatenet, Influence of the concentration of borohydride towards hydrogen production and escape for borohydride oxidation reaction on Pt and Au electrodes – experimental and modelling insights, J. Power Sources 375 (2018) 300–309.

[15] J.M. Nurul, A. Choudhury, Y. Sahai, A comprehensive review of direct borohydride fuel cells, Renew. Sust. Energy Rev. 14 (2010) 183–199.

[16] A. Zadick, J.F. Petit, V. Martin, L. Dubau, U.B. Demirci, C. Geantet, M. Chatenet, Ubiquitous borane fuel electrooxidation on Pd/C and Pt/C electrocatalysts: toward promising direct hydrazine-borane fuel cells, ACS Catal. 8 (2018) 3150–3163.

[17] S. Pylypko, A. Zadick, M. Chatenet, P. Miele, M. Cretin, U.B. Demirci, A preliminary study of sodium octahydrotriborate NaB_3H_8 as potential anodic fuel of direct liquid fuel cell, J. Power Sources 286 (2015) 10–17.

[18] F. Klanberg, E.L. Muetterties, Chemistry of boranes. XXVII. New polyhedral borane anions, $B_9H_9^{2-}$ and $B_{11}H_{11}^{2-}$, Inorg. Chem. 5 (1966) 1955–1960.

[19] D. Gabel, S. Mai, O. Perleberg, The formation of boron–carbon bonds to closo-decaborate(2–) and closo-dodecaborate(2–)), J. Organomet. Chem. 581 (1999) 45–50.

[20] W.I. Lipscomb, A.R. Pitochelli, M.F. Hawthorne, Probable structure of the $B_{10}H_{10}^{2-}$ anion, J. Am. Chem. Soc. 81 (1959) 5833–5834.

[21] E.L. Muetterties, J.H. Balthis, Y.T. Chia, W.H. Knoth, H.C. Miller, Chemistry of boranes. VIII. Salts and acids of $B_{10}H_{10}^{2-}$ and $B_{12}H_{12}^{2-}$, Inorg. Chem. 3 (1964) 444–451.

[22] D. Reed, The role of NMR in boron chemistry, Chem. Soc. Rev. 22 (1993) 109–116.

[23] T. Ruman, A. Kuśnierz, A. Jurkiewicz, A. Leś, W. Rode, The synthesis, reactivity and ^1H NMR investigation of the hydroxyborohydride anion, Inorg. Chem. Commun. 10 (2007) 1074–1078.

[24] E.S. Shubina, E.V. Bakhmutova, A.M. Filin, I.B. Sivaev, L.N. Teplitskaya, A.L. Chistyakov, I.V. Stankevich, V.I. Bakhmutov, V.I. Bregadze, L.M. Epstein, Dihydrogen bonding of decahydro-closo-decaborate(2–) and dodecahydro-closo-dodecaborate(2–)

anions with proton donors: experimental and theoretical investigation, J. Organomet. Chem. 657 (2002) 155–162.

[25] V.K. Skachkova, L.V. Goeva, A.V. Grachev, V.V. Avdeeva, E.A. Malinina, A.Yu. Shaulov, A.A. Berlin, N.T. Kuznetsov, Thermal and thermo-oxidative properties of the decahydro-closo-decaborate anion $B_{10}H_{10}^{2-}$ in a silicate matrix, Inorg. Mater. 51 (2015) 736–740.

[26] K. Hofmann, B. Albert, Crystal strcutures of $M_2[B_{10}H_{10}]$ (M = Na; K; Rb) via real-space simulated annealing powder techniques, Z. Kristallogr. 220 (2005) 143–146.

[27] H. Wu, W.S. Tang, W. Zhou, V. Stavila, J.J. Rush, T.J. Udovic, The structure of monoclinic $Na_2B_{10}H_{10}$: a combined diffraction, spectroscopy, and theoretical approach, Cryst. Eng. Commun. 17 (2015) 3533–3540.

[28] V. Petricek, M. Dusek, L. Palatinus, Crystallographic computing system JANA2006: general features, Z. Kristallogr. 3 (2014) 345–352.

[29] B.L. Chamberland, E.L. Muetterties, Chemistry of boranes. XVIII. Oxidation of $B_{10}H_{10}^{2-}$ and its derivatives, Inorg. Chem. 3 (1964) 1450–1456.

[30] A. Kaczmarczyk, G.B. Koiski, W.P. Townsend, Oxidative degradation of polyhedral boranes, J. Am. Chem. Soc. 87 (1965) 1413–1413.

[31] P. Rodriguez, M.T.M. Koper, Electrocatalysis on gold, Phys. Chem. Chem. Phys. 16 (2014) 13583–13594

[32] M. Chatenet, M.B. Molina-Concha, J.P. Diard, First insights into the borohydride oxidation reaction mechanism on gold by electrochemical impedance spectroscopy, Electrochim. Acta 54 (2009) 1687–1693.

[33] D.R. Smith, E.B. Rupp, D.F. Shriver, The mechanisms of electrolytic reduction for decaborane(14), $B_{10}H_{14}$, in an aprotic solvent. II. The second reduction step and the reduction of decaboran(13)ate(−1), $B_{10}H_{13}^{-1}$, J. Am. Chem. Soc. 89 (1967) 5568–5573.

[34] C. Grimmer, M. Grandi, R. Zacharias, B. Cermenek, H. Weber, C. Morais, T.W. Napporn, S. Weinberger, A. Schenk, V. Hacker, The electrooxidation of borohydride: A mechanistic study on palladium (Pd/C) applying RRDE, ^{11}B-NMR and FTIR, Appl. Catal. B: Env. 180 (2016) 614–621.

[35] E. Sanli, B.Z. Uysal, M.L. Aksu, The oxidation of $NaBH_4$ on electrochemicaly treated silver electrodes, Int. J. Hydrogen Energy 33 (2008) 2097–2104.

[36] M. Chatenet, F. Micoud, I. Roche, E. Chainet, Kinetics of sodium borohydride direct oxidation and oxygen reduction in sodium hydroxide electrolyte: Part I. BH_4^- electro-oxidation on Au and Ag catalysts, Electrochim. Acta 51 (2006) 5459–5467.

[37] G. Rostamikia, M.J. Janik, Direct borohydride oxidation: mechanism determination and design of alloy catalysts guided by density functional theory, Energy Environ. Sci. 3 (2010) 1262–1274.

[38] G. Rostamikia, R.J. Patel, I.. Merino-Jimenez, M. Hickner, M.J. Janik, Electrocatalyst design for direct borohydride oxidation guided by first principles, J. Phys. Chem. C 121 (2017) 2872–2881.

[39] D. Duan, H. Liu; Q. Wang, Y. Wang, S. Liu, Kinetics of sodium borohydride direct oxidation on carbon supported Cu-Ag bimetallic nanocatalysts, Electrochim. Acta 198 (2016) 212–219.

[40] B. Molina Concha, M. Chatenet, Direct oxidation of sodium borohydride on Pt, Ag and alloyed Pt–Ag electrodes in basic media. Part I: Bulk electrodes, Electrochim. Acta 54 (2009) 6119–6129.

[41] U.B. Demirci, Direct liquid-feed fuel cells: Thermodynamic and environmental concerns, J. Power Sources 169 (2007) 239–246.